

## Article

# H-Terminated Diamond MOSFETs on High-Quality Diamond Film Grown by MPCVD

Wenxiao Hu <sup>1</sup>, Xinxin Yu <sup>1,2,\*</sup>, Tao Tao <sup>1,\*</sup>, Kai Chen <sup>1</sup>, Yucong Ye <sup>1</sup>, Jianjun Zhou <sup>3</sup>, Zili Xie <sup>1</sup>, Yu Yan <sup>1</sup>, Bin Liu <sup>1,\*</sup> and Rong Zhang <sup>1</sup>

<sup>1</sup> Jiangsu Provincial Key Laboratory of Advanced Photonic and Electronic Materials, School of Electronic Science and Engineering, Nanjing University, Nanjing 210093, China

<sup>2</sup> CETC Key Laboratory of Carbon-Based Electronics, Nanjing Electronic Devices Institute, Nanjing 210016, China

<sup>3</sup> National Key Lab of Solid-State Microwave Devices and Circuits, Nanjing Electronic Devices Institute, Nanjing 210016, China; jjzhouhawk@163.com

\* Correspondence: yuxx711@126.com (X.Y.); ttiao@nju.edu.cn (T.T.); bliu@nju.edu.cn (B.L.)

**Abstract:** Diamond-based transistors have been considered as one of the best choices due to the numerous advantages of diamond. However, difficulty in the growth and fabrication of diamond needs to be addressed. In this paper, high quality diamond film with an atomically flat surface was grown by microwave plasma chemical vapor deposition. High growth rate, as much as 7  $\mu\text{m}/\text{h}$ , has been acquired without nitrogen doping, and the root mean square (RMS) of the surface roughness was reduced from 0.92 nm to 0.18 nm by using a pre-etched process. H-terminated diamond MOSFETs were fabricated on a high-quality epitaxial diamond layer, of which the saturated current density was enhanced. The hysteresis of the transfer curve and the shift of the threshold voltage were significantly reduced as well.

**Keywords:** single-crystal; diamond; MPCVD; H-diamond; MOSFET



**Citation:** Hu, W.; Yu, X.; Tao, T.; Chen, K.; Ye, Y.; Zhou, J.; Xie, Z.; Yan, Y.; Liu, B.; Zhang, R. H-Terminated Diamond MOSFETs on High-Quality Diamond Film Grown by MPCVD. *Crystals* **2023**, *13*, 1221. <https://doi.org/10.3390/cryst13081221>

Academic Editor: Giuseppe Prestopino

Received: 29 June 2023

Revised: 28 July 2023

Accepted: 29 July 2023

Published: 8 August 2023



**Copyright:** © 2023 by the authors. Licensee MDPI, Basel, Switzerland. This article is an open access article distributed under the terms and conditions of the Creative Commons Attribution (CC BY) license (<https://creativecommons.org/licenses/by/4.0/>).

## 1. Introduction

Recently, diamond has been considered as a promising wide-bandgap semiconductor material for electronic device applications due to its excellent thermal conductivity and electrical properties [1,2]. However, the difficulty of N-type doping limits the development of diamond-based electronic devices. Fortunately, high density two-dimensional hole gas (2DHG) can be acquired by hydrogen-terminated diamond film, which has been widely investigated because of its large critical breakdown electric field [3,4]. To date, high-crystal-quality diamond can be acquired by high-press high-temperature (HPHT) [5] or microwave plasma chemical vapor deposition (MPCVD) [6] methods. However, usually an epitaxial diamond layer with a macro-bunching step surface morphology cannot be used to fabricate the devices directly [7]. Devices fabricated directly onto a rough epitaxial layer usually have a worse performance [8]. Therefore, the diamond substrate needs to undergo a Chemical Mechanical Polishing (CMP) process before the fabrication of the diamond devices [9–11]. However, it is still difficult to produce a smooth diamond substrate by CMP, which is because of the natural hardness of diamond material. On the other hand, CMP process will also cause surface damage [12]. Therefore, the performance of diamond-based electronic devices on a polished substrate is still weak. In order to remove the surface defects introduced by the polishing process, a pre-etching process need to be added before the diamond epitaxy. The pre-etching process will introduce etch-pits on the diamond substrate, and the etch-pits usually can only be refilled under a high growth rate. In some references (100), face-diamond epitaxial film with a smooth surface has been obtained by quite a low growth rate. For instance, H. Okushi et al. [6] realized the 2D step-flow growth of diamonds with roughness of less than 0.1 nm within a  $1 \times 1 \mu\text{m}^2$  area at a

growth rate less than 30 nm/h. It was reported that the disorientation angle with respect to the (100) plane must be lower than  $1.5^\circ$ . Currently, it is still hard to produce a high quality single-crystal diamond film with a flat and low root-mean-square (RMS) surface at a high growth rate, especially on diamond substrates with a high disorientation angle. It is essential to the fabrication of diamond devices. Figure 1 lists the problems encountered when diamond substrates are used to fabricate devices. In this paper, high quality epitaxial diamond films with low surface roughness were grown by MPCVD. Hydrogen-terminated diamond MOSFETs with enhanced device performance were fabricated on such epitaxial diamond film.

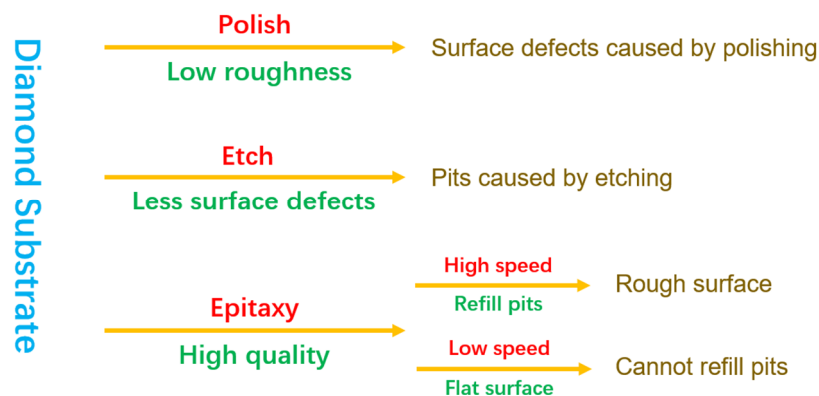


**Figure 1.** Problems encountered in fabricating devices with diamond substrates.

## 2. Experimental Section

We used (100)-oriented CVD diamond substrates in this paper. The size of the substrates is 10 mm  $\times$  10 mm, and the (100) face disorientation angle is  $3^\circ$ . The substrates were provided by the EDP Corporation, Japan. Firstly, the diamond substrates were cleaned in 60 degrees aqua regia for 40 min, and then ultrasonically cleaned in acetone, alcohol, and deionized water for 15 min each before growth. The MPCVD system for the growth of diamond layers is series ARDIS-300 from Optosystems, Ltd. [13,14]. Before the growth, the reactor chamber was pumped to high-vacuum  $2 \times 10^{-5}$  torr by using a mechanical pump and a turbomolecular pump (EDWARDS Next2400) in order to reduce residual nitrogen gas. Importantly, the substrate was pre-etched in hydrogen plasma to reduce the CMP damage and impurities, because it has been found that pre-etching treatment before growth can give birth to a smooth surface morphology of CVD diamond film [15]. Subsequently, the growth of the epitaxial diamond layer started. The microwave power, pressure in the reaction chamber, and the time in pre-etching and growth process, were set as 3200 W/3600 W, 250 torr/300 torr, and 30 min/1 h, respectively. The gas flow rate ratio of  $\text{CH}_4/\text{H}_2$  was 2%. In this work, the height of the sample could be adjusted vertically during growth, which is vital for the pre-etching process. It is because of this that the distance between the plasma and the diamond surface will significantly affect the nuclear center on the surface of the diamond substrate.

After the growth of the diamond layer, a thin hydrogen-terminated diamond layer was formed for the fabrication of the MOSFET device. The diamond sample was cleaned by  $\text{H}_2\text{SO}_4/\text{HNO}_3$  solution first, and then reloaded in the MPCVD chamber and undergoing a fast treatment process by hydrogen plasma. The microwave power and the pressure in the reaction chamber were set as 2600 W and 150 torr. Finally, the diamond was exposed to the air atmosphere for one day to form 2DHG. Next, a 50 nm Au film was deposited on the diamond surface to form ohmic contacts by electron beam (EB) evaporation. The source, drain, and channel regions were protected by the photoresist. The Au in the unmasked area was removed to the potassium iodide (KI) solution. Subsequently, the diamond was exposed to an oxygen plasma condition for 5 min to achieve device electric isolations. The spacing between the source and drain was realized by a second photolithography process.

Finally, a 50 nm  $\text{Al}_2\text{O}_3$  gate dielectric was deposited by atomic layer deposition (ALD). The reference sample was also fabricated under the same conditions on a polished diamond substrate. Figure 2 demonstrates the schematic structure, the photo and SEM image of the H-diamond based MOSFET fabricated in this work.

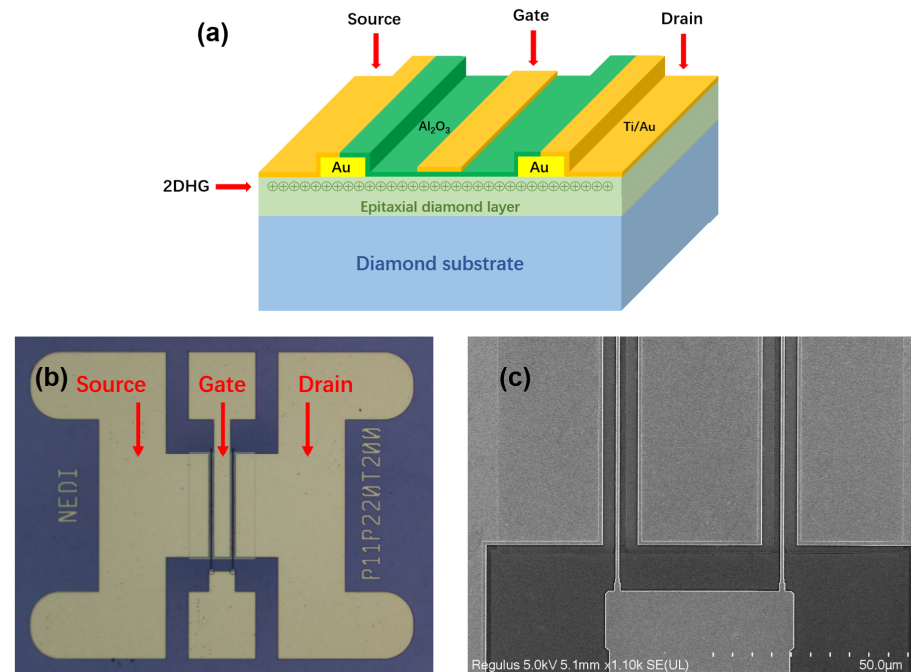


**Figure 2.** (a) The schematic cross-section structure; (b) optical microscope photo; and (c) SEM image of the H-diamond MOSFET.

The surface morphology was captured by the optical microscope and Atomic Force Microscope (AFM). The AFM was an NT-MDT NTEGRA Spectra II, scanned in tapping mode. The crystal quality of the diamond was measured by Raman, XRD and photoluminescence (PL). The PL spectra were collected using a HORIBA iHR 320 with a spectral resolution of 0.06 nm, optically pumped by a 514 nm semiconductor laser. All the direct current characteristics were conducted by using an Agilent B1500A system.

### 3. Results and Discussion

The Raman spectra of the diamond substrate and the epitaxial diamond layer are shown in Figure 3a. The Raman spectra of the diamond substrate peak at  $1334.5\text{ cm}^{-1}$ , while that of the epitaxial diamond layer exhibit little Raman peak shift, indicating little stress accumulation. The FWHM of the original diamond substrate was  $3.11\text{ cm}^{-1}$  and it was reduced to  $2.58\text{ cm}^{-1}$  after one hour of growth. The intensity of the peak is also stronger after epitaxy. The (400) XRD rocking curves in Figure 3b show similar results. Diamond after epitaxy has an FWHM of  $0.015^\circ$ , which is lower than the  $0.017^\circ$  of the diamond substrate. Enhanced crystal quality was realized after the epitaxy process. The thickness of the epitaxial layer is about  $7\text{ }\mu\text{m}$ .

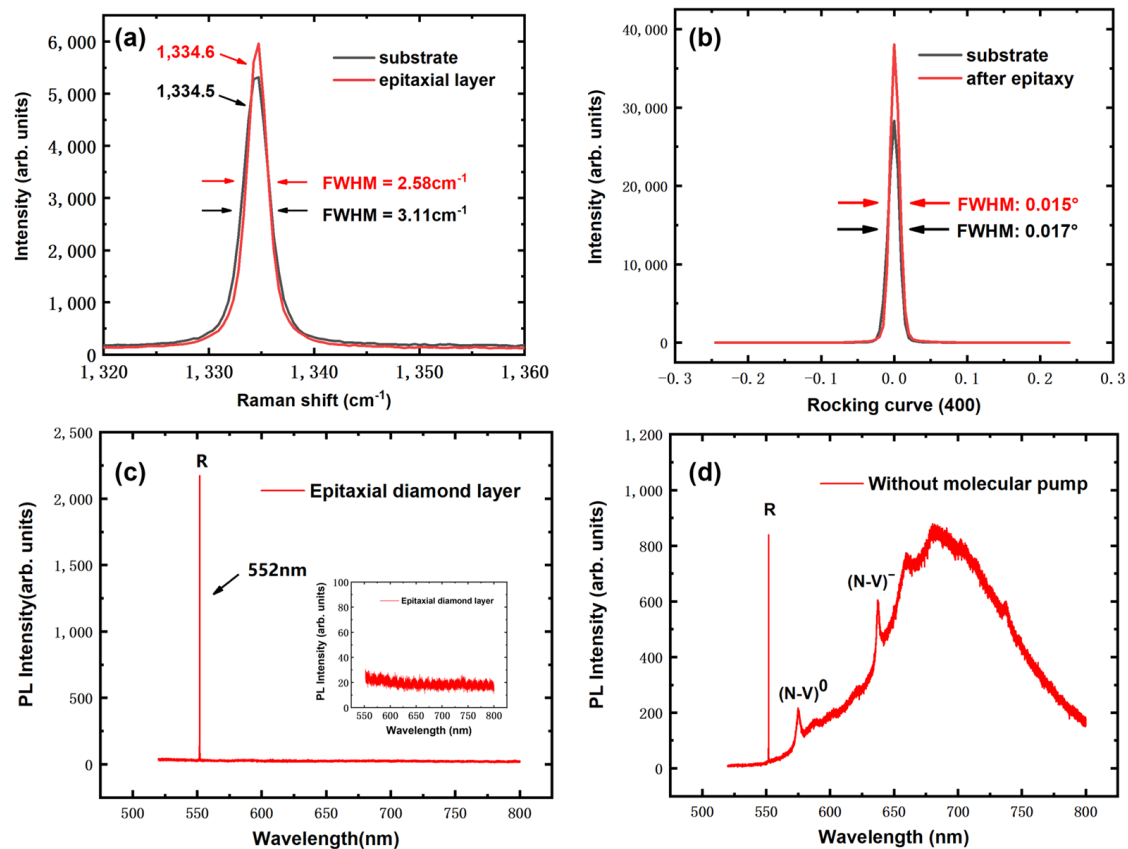


**Figure 3.** (a) Raman spectra of the diamond substrate and the thick epitaxial layer; (b) XRD results of the epitaxial diamond layer; (c,d) PL spectra of the epitaxial diamond layer.

Figure 3c demonstrates the PL spectra of the CVD diamond samples, where a 514 nm wavelength laser was used as the excitation light source. The sharp peak at a wavelength of 552 nm corresponds to the Raman peak of the diamond layer. As shown in the insert picture of Figure 3c, no other impurities-related emission is found, indicating a high purity in our growth process. The growth rate of the diamond layer is estimated to be  $\sim 7 \mu\text{m/h}$ . Normally, a high growth rate of CVD diamond can be achieved by nitrogen doping during the growth. However, it might introduce nitrogen related defects in CVD diamond layer, which have a negative influence on the electronic device's performance. In this work, the high growth rate was acquired by using high microwave power and high pressure in the growth process. No peaks at 575 nm and 637 nm were found, which correspond to the  $(\text{N-V})^0$  and  $(\text{N-V})^-$  peaks and appear as a result of the low-purity CVD process [16]. Figure 3d shows an epitaxial diamond sample, on which was only used a mechanical pump to evacuate the reaction chamber before growth. Although there was no intentional nitrogen doping during the growth process, its PL spectra still show strong peaks associated with nitrogen defects and a molecular pump can help eliminate the effects of nitrogen impurities. As a result, undoped single crystal diamonds with smooth surfaces and better crystal quality have been obtained, supporting the fabrication of diamond MOSFET devices.

Normally, diamond epitaxial layers have a macro-bunching step morphology [6] due to their step formation energies [7]. A rough surface is not beneficial to the fabrication of electrodes and the performance of the devices. Therefore, diamond devices are usually fabricated on a polished diamond substrate. However, surface defects and damage will be generated in the polishing process, which have a major influence on the performance of devices fabricated on a polished diamond substrate. A pre-etching process, as shown in Figure 4, can remove the surface defects. Under an H-plasma environment, diamond  $\{113\}$  faces have higher etching rates compare to other faces, such as  $\{111\}$  and  $\{100\}$  faces [17].

Etching pits will appear at the area of the surface defects. Diamond substrates with etching pits are also not conducive to the fabrication of devices. Therefore, only a flat-surface diamond epitaxial layer can eliminate the adverse effects of surface defects and etching pits on the device. The etching pits will be recovered in a several microns thick epitaxial layer due to the higher growth rate of {113} than {100} faces, as shown in Figure 4. In past references, atomically flat diamond epitaxial layers can only be realized in an extremely low growth rate [6,18,19]. It is not practical in the semiconductor industry. In our previous works [20], a smooth diamond epitaxial layer was achieved by optimizing the conditions of the pre-etching process. It is important to mention that the distance between the diamond surface and the plasma ( $d_{DP}$ ) should be precisely controlled during the pre-etching process.

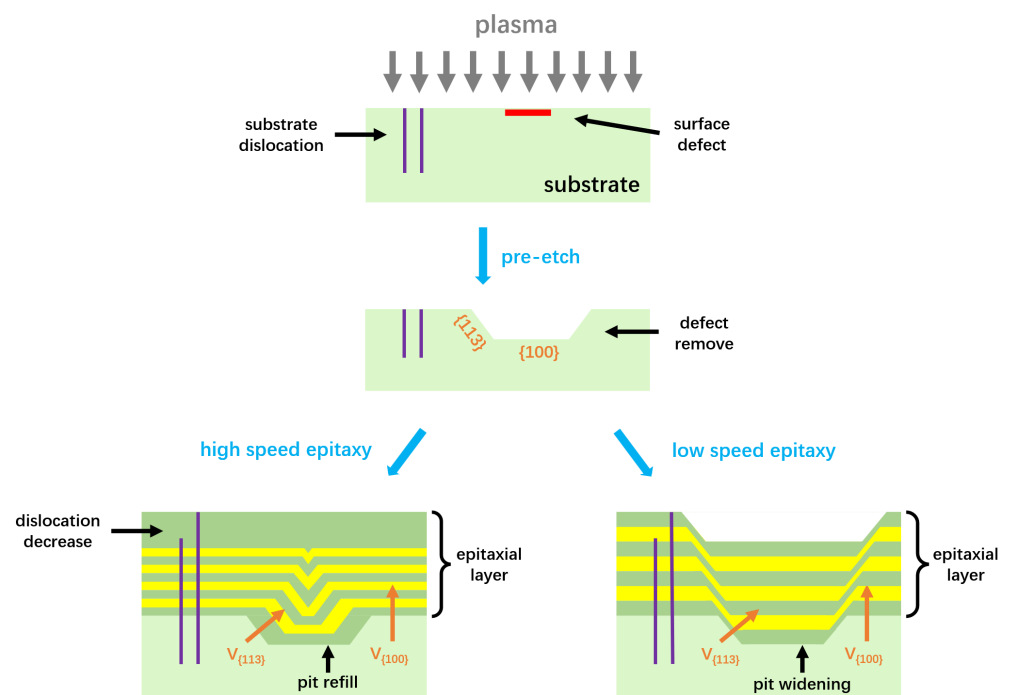


**Figure 4.** Sketch of the epitaxial process with different growth rates.

Etching pits with different sizes were found on the diamond substrate after the H-plasma etching process, as demonstrated in Figure 5a, which came from the diamond itself and the polishing process. The substrates used in Figure 5 come from the Zhengzhou Sino-Crystal Diamond Co., Ltd., Zhengzhou, China. These substrates have many more etching pits after the H-plasma etching process compared to the substrates from EDP Corporation, Japan. Figure 5d shows several etching pits of different sizes. They are all rectangular in shape and the rectangular edges are parallel to each other, indicating the effect of crystal orientation on the etching rate. After epitaxy with a high growth rate ( $\sim 20 \mu\text{m}/\text{h}$ ) using a 6%  $\text{CH}_4/\text{H}_2$  ratio for 20 min, etching pits were successfully recovered and a flat surface was acquired, as shown in Figure 5b,e. Macro-bunching step morphology was also absent by using a low growth rate (0.5%  $\text{CH}_4/\text{H}_2$  ratio). However, the etching pits might become larger as shown in Figure 5c. The post-epitaxial pits, as presented in Figure 5f, are significantly larger and deeper than the pre-epitaxial etching pits. The low growth rate of {113} face is not beneficial for the pits' recovery, as shown in Figure 4. Normally, pits' recovery can be achieved by nitrogen doping during the growth [17]. However, it might introduce nitrogen related defects in the CVD diamond layer, which has negative influences on the electronic device's performance. Therefore, it is important to acquire a high growth rate for realizing the atomically flat epitaxial diamond layer. The reported growth rates and roughness of the diamond's epitaxial layer with a flat surface morphology are summarized and shown in Figure 6 [6,12,18–21]. H. Okushi et al. have realized diamond 2D step flow

growth and a roughness  $R_a$  of less than 0.1 nm in  $1 \mu\text{m} \times 1 \mu\text{m}$  area, but the growth rate was only less than 30 nm/h. G. Bogdan et al. achieved a smooth diamond epitaxial layer with a higher growth rate (2.5~4.5  $\mu\text{m}/\text{h}$ ), but the roughness  $R_a$  also increased to 0.5~0.8 nm in a  $5 \mu\text{m} \times 5 \mu\text{m}$  area. As the growth rate increases, the surface roughness becomes larger, as indicated by the dash line. In these papers, the diamonds' substrates usually also needed a low disorientation angle, at least lower than  $1.5^\circ$  with respect to the (100) plane. This may increase the cost of the diamond substrate and the low growth rate may also not be enough to refill the etch pits. In this paper and our previous work, the growth rate was improved obviously, and the surface roughness was also reduced. With the growth rate as high as 7~30  $\mu\text{m}/\text{h}$ , the RMS roughness can reach as low as 0.2~0.5 nm in  $5 \mu\text{m} \times 5 \mu\text{m}$  area. The high growth rate was acquired by using high temperature and high flow ratio of  $\text{CH}_4/\text{H}_2$  during the growth process. N-related peaks cannot be found in the PL result, as shown in Figure 3c. Undoped single-crystal diamonds with atomically flat surfaces and high crystal quality have been obtained, providing support for the fabrication of diamond-based MOSFET devices. Therefore, better device performance can be realized by epitaxial layers attributed to reduced surface defects during growth. With the thickness of epitaxial layers increased, etching pits and polishing bunches have also been decreased, further improving the device's performance.

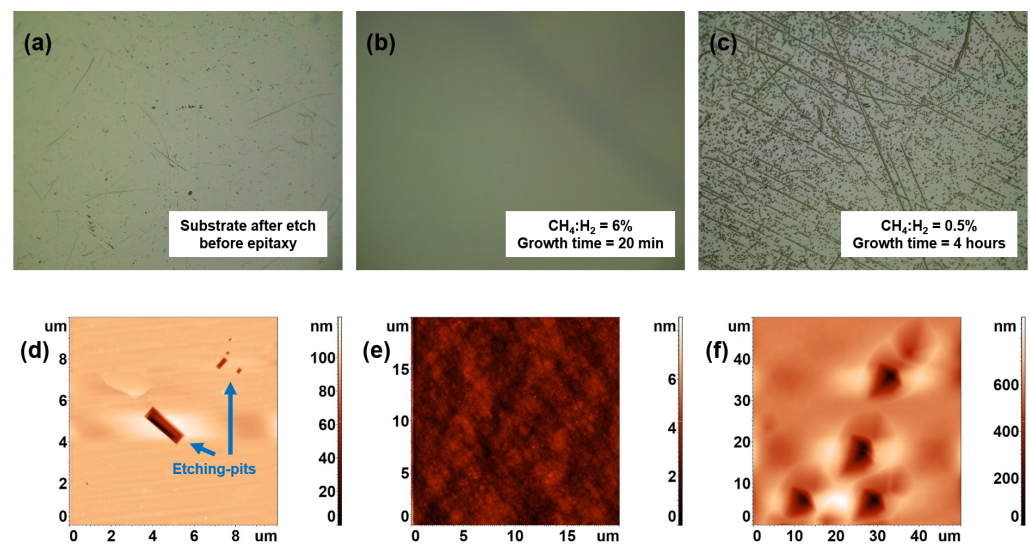


**Figure 5.** The surface morphology of the diamond substrate after etching process (a,d); epitaxy diamond layer with a high growth rate (b,e); and with a low growth rate (c,f).

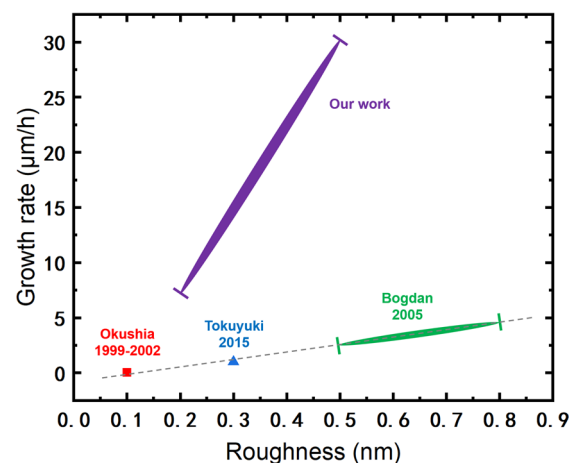


**Figure 6.** The roughness and the growth rate of the flat diamond epitaxial layer [6,12,18–21].

Three MOSFETs were fabricated on a polished diamond substrate and epitaxial diamond layers, respectively. Sample 1 is a reference sample fabricated on a polished diamond substrate. Sample 2 has a thin epitaxial layer ( $\sim 3 \mu\text{m}$ ) with 0.5-h growth time and sample 3 has a thick epitaxial layer ( $\sim 7 \mu\text{m}$ ) with 1-h growth time. Samples 2 and 3 used a same growth condition, and the  $\text{CH}_4/\text{H}_2$  ratio used in samples 2 and 3 was 2%. The AFM results of these three samples are shown in Figure 7a–c. Parallel polishing grooves could be found on the surface of the substrate and it had an RMS of 0.92 nm in a  $5 \mu\text{m} \times 5 \mu\text{m}$  region. After 0.5 h of growth, the RMS was reduced to 0.52 nm, and it could be further reduced down to 0.18 nm with the increased epitaxial layer. The surface of the epitaxial layer was much smoother than that of the original diamond substrate.

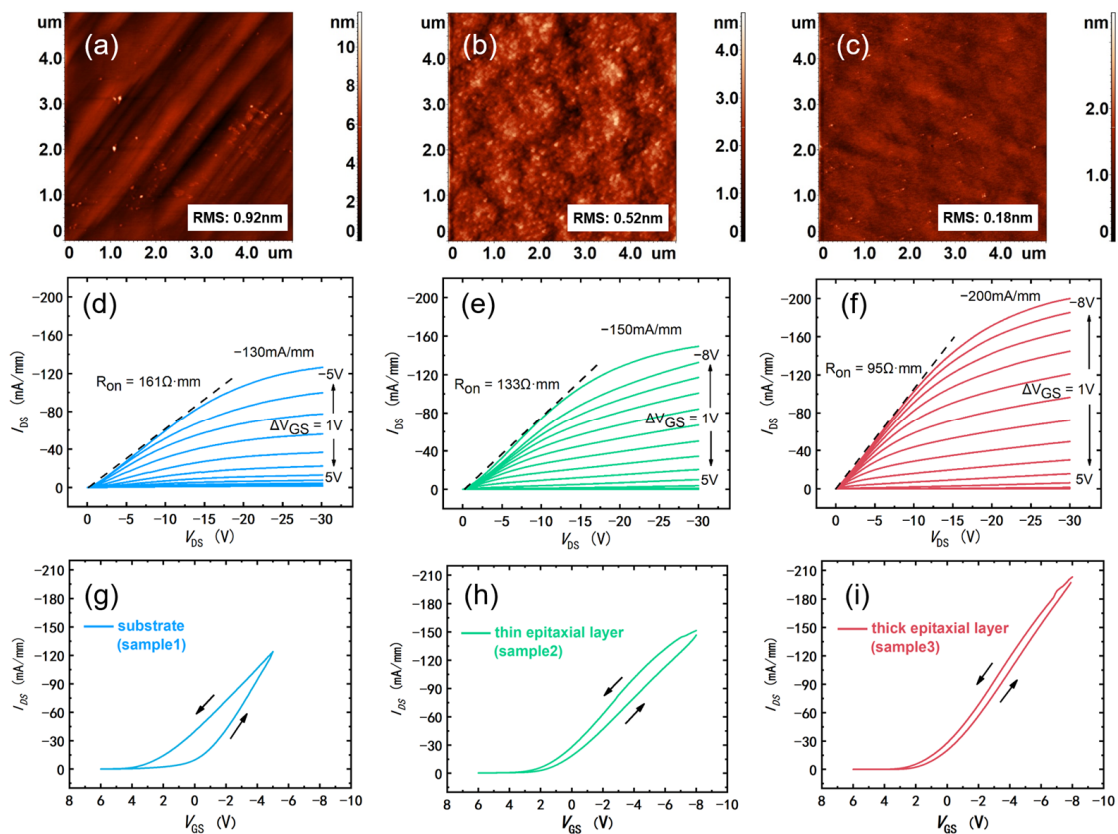


**Figure 7.** The AFM results, direct current output characteristics and the transfer characteristics of the MOSFETs using a diamond substrate (a,d,g), and a thin (b,e,h) and thick (c,f,i) epitaxial diamond layer. The dotted line in (d–f) are the tangent line of the direct current. The arrows in (g–i) represent the scanning direction.

The current output characteristics and the transfer characteristics of the H-diamond MOSFETs are shown in Figure 7. The reference MOSFET sample 1, fabricated on the polished diamond substrate, was measured under the  $V_{GS}$  ranging from  $-5 \text{ V}$  to  $5 \text{ V}$ , of which the saturation current density was  $\sim 130 \text{ mA/mm}$ . Meanwhile, the MOSFET samples 2 and 3, fabricated on the epitaxial diamond layers, were measured under the  $V_{GS}$  ranging from  $-8 \text{ V}$  to  $5 \text{ V}$  and had a higher saturation current density of  $\sim 150 \text{ mA/mm}$  and  $\sim 200 \text{ mA/mm}$ , respectively. After the epitaxy, 54% improvement was acquired with respect to the reference sample, and  $R_{on}$  was also decreased from  $161 \Omega \cdot \text{mm}$  to  $95 \Omega \cdot \text{mm}$ . The transfer characteristics shown in Figure 7g–i further prove that the MOSFET fabricated on a thicker epitaxial diamond layer could have a better performance. For the MOSFET on the original diamond substrate, the hysteresis of transfer curve is large, and the threshold voltage will drift seriously. Significant improvement can be realized in MOSFETs on the epitaxial diamond layer, as shown in Figure 7h–i, especially on a thicker epitaxial layer.

During testing, especially at turn-off, if the device's substrate contains more defects, the more likely its carriers will be captured by the trap. Thus, the current drops back during the scan. A larger hysteresis indicates more substrate defects. Obviously, an epitaxial diamond layer with a smooth surface is beneficial for MOSFET devices compared to the CMP polished diamond substrate.

#### 4. Conclusions

In this paper, a single-crystal diamond epitaxial layer with a smooth surface morphology was grown by MPCVD using a pre-etching process. Etching pits were recovered, and an atomically flat diamond epitaxial layer was realized at a high growth rate of  $\sim 7 \mu\text{m/h}$ . H-terminated diamond MOSFETs were fabricated on the epitaxial layer, for which the performance was significantly improved with respect to the original diamond substrate. This further proves that surface morphology and defects have important impacts on the performance of H-diamond MOSFETs. The optimized epitaxial diamond layer with a flat surface morphology can provide a feasible solution for diamond-based devices.

**Author Contributions:** Conceptualization, W.H.; Data curation, W.H. and X.Y.; Funding acquisition, T.T., J.Z., Z.X., Y.Y. (Yu Yan), B.L. and R.Z.; Investigation, W.H., X.Y., K.C. and Y.Y. (Yucong Ye); Project administration, B.L.; Resources, J.Z., Z.X., B.L. and R.Z.; Supervision, B.L.; Validation, W.H.; Visualization, W.H. and X.Y.; Writing—original draft, W.H.; Writing—review and editing, T.T. and B.L. All authors have read and agreed to the published version of the manuscript.

**Funding:** This work is supported by the National Key R&D Program of China (2021YFB3601600), the National Nature Science Foundation of China (61974062, 62074077, 62004104, 61921005, 61974031, 61904068), the Leading-edge Technology Program of Jiangsu Natural Science Foundation (BE2021008-2), the Fundamental Research Foundation for the Central Universities, Collaborative Innovation Center of Solid-State Lighting and Energy-Saving Electronics, and the Foundation of Lohua Chip-Display Technology Development Co., Ltd. (2022320116000031).

**Data Availability Statement:** The data that support the findings of this study are available within the article.

**Conflicts of Interest:** The authors declare no conflict of interest.

#### References

1. Isberg, J.; Hammersberg, J.; Johansson, E.; Wikström, T.; Twitchen, D.J.; Whitehead, A.J.; Coe, S.E.; Scarsbrook, G.A. High Carrier Mobility in Single-Crystal Plasma-Deposited Diamond. *Science* **2002**, *297*, 1670–1672. [[CrossRef](#)] [[PubMed](#)]
2. Balmer, R.S.; Brandon, J.R.; Clewes, S.L.; Dhillon, H.K.; Dodson, J.M.; Friel, I.; Inglis, P.N.; Madgwick, T.D.; Markham, M.L.; Mollart, T.P.; et al. Chemical vapour deposition synthetic diamond: Materials, technology and applications. *J. Phys. Condens. Matter* **2009**, *21*, 364221. [[CrossRef](#)] [[PubMed](#)]
3. Yu, X.; Hu, W.; Zhou, J.; Liu, B.; Tao, T.; Kong, Y.; Chen, T.; Zheng, Y. 1 W/mm Output Power Density for H-Terminated Diamond MOSFETs With  $\text{Al}_2\text{O}_3/\text{SiO}_2$  Bi-Layer Passivation at 2 GHz. *IEEE J. Electron Devices Soc.* **2020**, *9*, 160–164. [[CrossRef](#)]
4. Yu, X.; Hu, W.; Zhou, J.; Wu, Y.; Tao, R.; Liu, B.; Tao, T.; Wei, Z.; Kong, Y.; Ye, J.; et al. 1.26 W/mm Output Power Density at 10 GHz for  $\text{Si}_3\text{N}_4$  Passivated H-Terminated Diamond MOSFETs. *IEEE Trans. Electron Devices* **2021**, *68*, 5068–5072. [[CrossRef](#)]
5. Yin, L.-W.; Li, M.-S.; Sun, D.-S.; Li, F.-Z.; Hao, Z.-Y. Some aspects of diamond crystal growth at high temperature and high pressure by TEM and SEM. *Mater. Lett.* **2002**, *55*, 397–402. [[CrossRef](#)]
6. Okushi, H.; Watanabe, H.; Ri, S.; Yamanaka, S.; Takeuchi, D. Device-grade homoepitaxial diamond film growth. *J. Cryst. Growth* **2002**, *237–239*, 1269–1276. [[CrossRef](#)]
7. Yang, H.X.; Xu, L.F.; Fang, Z.; Gu, C.Z.; Zhang, S.B. Bond-Counting Rule for Carbon and its Application to the Roughness of Diamond (001). *Phys. Rev. Lett.* **2008**, *100*, 026101. [[CrossRef](#)]
8. Zhang, X.; Matsumoto, T.; Nakano, Y.; Noguchi, H.; Kato, H.; Makino, T.; Takeuchi, D.; Ogura, M.; Yamasaki, S.; Nebel, C.E.; et al. Inversion channel MOSFET on heteroepitaxially grown free-standing diamond. *Carbon* **2020**, *175*, 615–619. [[CrossRef](#)]
9. Ueda, K.; Kasu, M.; Yamauchi, Y.; Makimoto, T.; Schwitters, M.; Twitchen, D.; Scarsbrook, G.; Coe, S. Diamond FET using high-quality polycrystalline diamond with  $f_{\text{sub T}}/f_{\text{max}}$  of 45 GHz and  $f_{\text{sub max}}/f_{\text{max}}$  of 120 GHz. *IEEE Electron Device Lett.* **2006**, *27*, 570–572. [[CrossRef](#)]
10. Yu, X.; Zhou, J.; Qi, C.; Cao, Z.; Kong, Y.; Chen, T. A High Frequency Hydrogen-Terminated Diamond MISFET With  $f_{\text{T}}/f_{\text{max}}$  of 70/80 GHz. *IEEE Electron Device Lett.* **2018**, *39*, 1373–1376. [[CrossRef](#)]
11. Yu, C.; Zhou, C.J.; Guo, J.C.; He, Z.Z.; Wang, H.X.; Cai, S.J.; Feng, Z.H. 650 mW/mm output power density of H-terminated polycrystalline diamond MISFET at 10 GHz. *Electron. Lett.* **2020**, *56*, 334–335. [[CrossRef](#)]

12. Teraji, T.; Yamamoto, T.; Watanabe, K.; Koide, Y.; Isoya, J.; Onoda, S.; Ohshima, T.; Rogers, L.J.; Jelezko, F.; Neumann, P.; et al. Homoepitaxial diamond film growth: High purity, high crystalline quality, isotopic enrichment, and single color center formation. *Phys. Status Solidi* **2015**, *212*, 2365–2384. [[CrossRef](#)]
13. Wang, X.; Duan, P.; Cao, Z.; Liu, C.; Peng, Y.; Hu, X. Homoepitaxy Growth of Single Crystal Diamond under 300 torr Pressure in the MPCVD System. *Materials* **2019**, *12*, 3953. [[CrossRef](#)] [[PubMed](#)]
14. Zhi, T.; Tao, T.; Liu, B.; Wang, X.; Hu, W.; Chen, K.; Xie, Z.; Zhang, R. High quality CVD single crystal diamonds grown on nanorods patterned diamond seed. *Diam. Relat. Mater.* **2021**, *119*, 108605. [[CrossRef](#)]
15. Tallaire, A.; Achard, J.; Silva, F.; Sussmann, R.S.; Gicquel, A.; Rzepka, E. Oxygen plasma pre-treatments for high quality homoepitaxial CVD diamond deposition. *Phys. Status Solidi* **2004**, *201*, 2419–2424. [[CrossRef](#)]
16. Ismagilov, R.; Malykhin, S.; Puzyr, A.; Loginov, A.; Kleshch, V.; Obraztsov, A. Single-Crystal Diamond Needle Fabrication Using Hot-Filament Chemical Vapor Deposition. *Materials* **2021**, *14*, 2320. [[CrossRef](#)]
17. Achard, J.; Silva, F.; Brinza, O.; Bonnin, X.; Mille, V.; Issaoui, R.; Kasu, M.; Gicquel, A. Identification of etch-pit crystallographic faces induced on diamond surface by H<sub>2</sub>/O<sub>2</sub> etching plasma treatment. *Phys. Status Solidi* **2009**, *206*, 1949–1954. [[CrossRef](#)]
18. Okushi, H. High quality homoepitaxial CVD diamond for electronic devices. *Diam. Relat. Mater.* **2001**, *10*, 281–288. [[CrossRef](#)]
19. Watanabe, H.; Takeuchi, D.; Yamanaka, S.; Okushi, H.; Kajimura, K.; Sekiguchi, T. Homoepitaxial diamond film with an atomically flat surface over a large area. *Diam. Relat. Mater.* **1999**, *8*, 1272–1276. [[CrossRef](#)]
20. Hu, W.; Chen, K.; Tao, T.; Yu, X.; Zhou, J.; Xie, Z.; Liu, B.; Zhang, R. High-rate growth of single-crystal diamond with an atomically flat surface by microwave plasma chemical vapor deposition. *Thin Solid Films* **2022**, *763*, 139571. [[CrossRef](#)]
21. Bogdan, G.; Nesládek, M.; D’Haen, J.; Maes, J.; Moshchalkov, V.V.; Haenen, K.; D’Olieslaeger, M. Growth and characterization of near-atomically flat, thick homoepitaxial CVD diamond films. *Phys. Status Solidi* **2005**, *202*, 2066–2072. [[CrossRef](#)]

**Disclaimer/Publisher’s Note:** The statements, opinions and data contained in all publications are solely those of the individual author(s) and contributor(s) and not of MDPI and/or the editor(s). MDPI and/or the editor(s) disclaim responsibility for any injury to people or property resulting from any ideas, methods, instructions or products referred to in the content.